

# The structure and deformation behaviour of poly(*p*-phenylene benzobisoxazole) fibres

R. J. YOUNG, R. J. DAY, M. ZAKIKHANI

*Polymer Science and Technology Group, Manchester Materials Science Centre, University of Manchester Institute of Science and Technology, P.O. Box 88, Manchester M60 1QD, UK*

The relationship between structure and mechanical properties in as-spun and heat-treated high modulus poly(*p*-phenylene benzobisoxazole) (PBO) fibres has been examined using a combination of electron microscopy, mechanical testing, and Raman microscopy. The structure of the fibres has been determined by obtaining longitudinal sections, and electron diffraction has shown that skin regions are significantly more oriented than the fibre cores. Heat treatment of the fibres at elevated temperatures produces an improvement in the level of crystallinity especially in core regions. Heat treatment also produces an increase in fibre modulus but for fibres heat treated at 650°C there is a significant decrease in strength compared with ones heat treated at 600°C. Well-defined intense Raman spectra were obtained from individual fibres and three main bands at 1280, 1540 and 1615 cm<sup>-1</sup> have been identified. All three bands are sensitive to the level of applied strain with the 1280 cm<sup>-1</sup> being the most sensitive, shifting by -7.9 cm<sup>-1</sup>/% strain for PBO fibres heat treated at 600°C. The dependence of the sensitivity of the position of the 1615 cm<sup>-1</sup> band to strain upon fibre structure has been examined in detail. The rate of shift of band position with strain increases with fibre modulus. It is shown that these shifts in Raman bands are a direct reflection of molecular deformation within the fibres.

## 1. Introduction

There is now considerable interest in producing polymers fibres with high degrees of strength and stiffness combined with good thermal stability, principally for use in high-performance composites. One of the first examples of this was the production of high-modulus fibres of aromatic polyamides such as poly(*p*-phenylene terephthalamide) (Kevlar) which can be made by the spinning of liquid-crystalline solutions [1, 2]. An important development of this technology has led to high-modulus and high-strength polymer fibres using heterocyclic rigid-rod polymers, again by spinning from liquid-crystalline solutions. Fibres have been produced from poly(*p*-phenylene benzobisthiazole) (PBT) with a modulus, after heat treatment, of 320 GPa [3, 4]. More recent work has shown that heat-treated fibres obtained from poly(*p*-phenylene benzobisoxazole) (PBO) can have modulus values of up to 370 GPa [5]. Such fibres are also reported to have strengths of over 3 GPa and elongations to failure of up to 2%. These levels of stiffness and strength combined with their compressive oxidative and thermal stabilities [3] and low specific gravities mean that they are extremely promising as reinforcing fibres for high-performance composites.

It has been found that well-defined Raman spectra can be obtained from fibres of a wide variety of high-modulus polymeric and non-polymeric fibres. When such fibres are deformed the frequencies of Raman-active bands tend to decrease by an amount,  $\Delta\nu$ ,

dependent upon the material, the band under consideration and the modulus of the material. The largest shifts have been found in polydiacetylene single crystals deformed parallel to the molecular axis where values of  $\Delta\nu$  in the order of -20 cm<sup>-1</sup>/% strain have been reported [6, 7] for triple band stretching. Large shifts of up to -12 cm<sup>-1</sup>/% have been reported for the Raman active bands in high-modulus fibres of PBT and for a given band the rate of shift is seen to depend upon the fibre modulus [8]. Shifts of up to -5 cm<sup>-1</sup>/% have been reported for the 1610 cm<sup>-1</sup> band of aromatic polyamide (aramid) fibres such as Kevlar [9, 10] where the rate of shift is again found to depend upon the modulus of the fibre [10]. Deformation in the aramid fibre is thought to take place by a combination of crystal stretching and crystal rotation [9] but the shifts of the Raman bands reflect only the stretching component which is higher in the high-modulus fibres. Deformation in the lower modulus fibres takes place predominantly by crystal rotation. Similar behaviour has also been found for inorganic fibres such as carbon fibres [11] and carbon containing silicon carbide fibres [12] where mechanical deformation of the fibre causes direct straining of the graphite planes [11, 12] which leads to shifts in the carbon 1580 cm<sup>-1</sup> band of the order of -10 cm<sup>-1</sup>/% strain.

As well as giving useful information about the effect of mechanical strain upon the internal molecular structure of the fibres, the Raman technique can also be used to follow the micromechanics of the

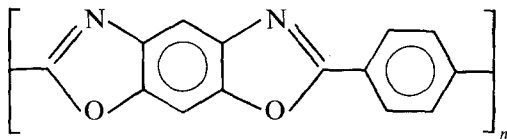
deformation of fibres within a composite because the fibres behave as though they contain an internal optical molecular strain gauge. So far, examples have been published of the measurement of fibre strain in polydiacetylene/epoxy composites [13, 14], Kevlar/epoxy composites [15] and carbon-fibre reinforced PEEK [16, 17].

This present study is concerned with structure/property relationships in as-spun PBO fibres and PBO fibres heat treated at 600 and 650°C. The structure and tensile properties of the fibre are first described. It is then shown that well-defined spectra can be obtained from the fibres and that the positions of the Raman-active bands depend upon the levels of stress applied to the fibres. The reasons for this behaviour are discussed and methods of exploiting the effect are then suggested.

## 2. Experimental details

### 2.1. Materials and characterization

The PBO fibres used in this study were supplied by the Materials Laboratory, Wright-Patterson Air Force Base, Ohio, USA and were based on the molecule



Three types of fibre were supplied. The first were straw-coloured "as-spun" (AS) fibres prepared from a solution in a concentrated acid. The second were higher modulus darker coloured fibres which had been given the optimum heat treatment of 600°C and the third set had been heat treated at 650°C.

Individual fibres were examined in a scanning electron microscope (Philips 525). They were cleaned using a solvent and then rendered conductive by sputter coating with a thin layer of gold. The fibres were examined to determine their geometry and diameter for calculation of stresses. The magnification of the microscope was calibrated accurately ( $\pm 2\%$ ) prior to these measurements.

Wide-angle X-ray scattering (WAXS) patterns were obtained from bundles of the different types of fibres using a flat-plate transmission geometry and nickel-filtered  $\text{CuK}\alpha$  radiation. This enabled the degree of perfection and level of molecular orientation in the different fibres to be compared.

Sections of the fibres were also examined in a transmission electron microscope (Philips 400T). Individual fibres were embedded in an epoxy resin and longitudinal sections were obtained using a microtome with the diamond knife cutting perpendicular to the fibre axis as described elsewhere for aromatic polyamides [18].

### 2.2. Mechanical testing

Individual PBO fibres were mounted across holes on paper cards using a slow setting, cold-curing, epoxy resin adhesive. Once the adhesive had set the pieces of card were mounted between fibre testing grips in a model 1121 Instron and the card edges were cut. Data for stress-strain curves were collected using an HP85

computer and also on chart paper. Load ranges of between 2 and 5 N were employed using a 5 N capacity load cell. The gauge length of the single-fibre specimens was about 50 mm and the fibre strain was determined from the cross-head displacement. A cross-head speed of  $1 \text{ mm min}^{-1}$  was used making an initial strain rate of  $3.3 \times 10^{-4} \text{ sec}^{-1}$ . At least 20 samples of each type of fibre were employed. All tests were carried out at  $23 \pm 1^\circ \text{C}$  and a relative humidity of  $50 \pm 5\%$ .

### 2.3. Raman microscopy

Raman spectra were obtained from individual PBO fibres using a Raman microscope system. This is based upon a SPEX 1403 double monochromator connected to a modified Nikon optical microscope. Spectra were obtained at a resolution of the order of  $\pm 5 \text{ cm}^{-1}$  using the 632.8 nm line of a 10 mW He/Ne laser. A  $\times 40$  objective lens with a numerical aperture of 0.65 was used and this gave a  $2 \mu\text{m}$  spot when focused (although the objective lens was generally defocused to reduce the possibility of damage through excessive heating). The laser beam was polarized parallel to the fibre axis for all measurements.

Spectra were obtained from fibres during deformation in a small straining rig which fitted directly on to the microscope stage. Individual fibres were fixed between aluminium foil tabs which were placed on to the aluminium blocks of the straining rig using either an epoxy or a cyanoacrylate adhesive, giving a gauge length of about 10 mm, which was measured accurately using the light microscope. The fibres were deformed by displacing the blocks using a micrometer attachment which could be read to  $\pm 0.005 \text{ mm}$ . This allowed a precision of the order of  $\pm 0.05\%$  for strain measurement. Raman spectra were obtained during deformation by scanning strong individual peaks between loading steps of 0.1% strain.

## 3. Results and discussion

### 3.1. Structure

The structure of the PBO fibres was determined using a combination of X-ray diffraction and electron microscopy. Using these techniques, no difference could be detected between the fibres heat treated at 600 and 650°C and so only the 600°C heat-treated fibres are described. Fig. 1 shows a scanning electron micrograph of 600°C heat-treated PBO fibres. The fibres were found and they ranged typically between

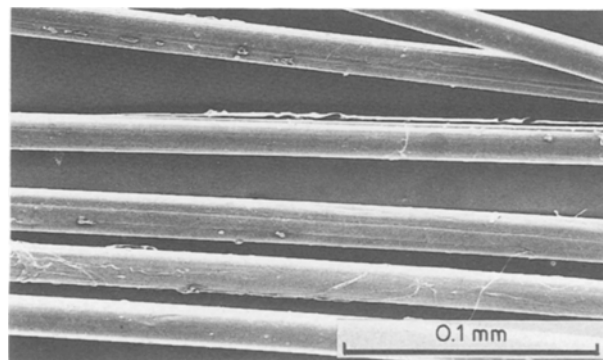


Figure 1 Scanning electron micrograph of PBO-600 fibres.

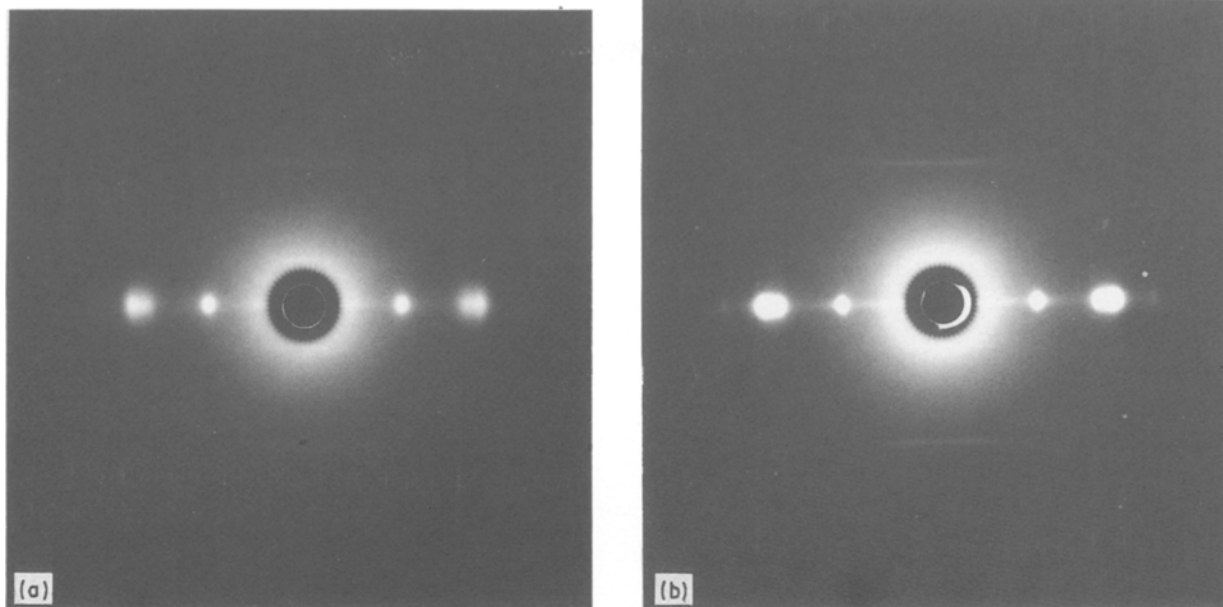


Figure 2 Wide-angle X-ray diffraction patterns of (a) PBO-AS, and (b) PBO-600.

12 and 18  $\mu\text{m}$  with a mean diameter of around 15  $\mu\text{m}$ . Measurements were made at a variety of positions on each fibre so that accurate values of fibre diameter could be obtained for the calculation of stresses. A few striations and kink bands could be seen on some fibres but in general they were seen to be relatively defect free.

WAXS patterns for the PBO-AS and PBO-600 types of fibre are shown in Fig. 2. The pattern for the as-spun fibre can be seen to consist of diffuse equatorial peaks which become sharper following heat treatment at 600°C. It should also be noted that well-defined off-axis first order ( $hkl$ ) reflections develop following the heat treatment. Krause *et al.* [5] pointed out that this indicated the development of three-dimensional crystallinity in PBO in contrast to PBT where no such off-axis ( $hkl$ ) reflections are found [19, 20]. The WAXS patterns are not as well-defined as those from aramid fibres which indicates that the three-dimensional order in heat-treated PBO is not as well-developed as in aramid fibres. Krause *et al.* [5] showed that the  $d$ -spacings remained relatively unchanged when PBO was heat treated indicating no significant

improvement in chain packing. On the other hand, they did note an increase in crystallite size and a reduction in disorder. Our results are in agreement with these observations.

Micrographs of longitudinal sections taken through PBO-AS and PBO-600 fibres are shown in Figs 3 and 4 for skin (a) and core (b) regions. The position of the selected-area aperture in each case is indicated. Selected-area diffraction patterns obtained from these regions are also presented with each micrograph. It can be seen that the structures consist of fibrils on the 100 nm to 200 nm scale although it is not clear as to whether or not they represent true structural features or have been formed during sectioning. Unlike aromatic polyamides [18], no periodic structure or banding could be seen on the 0.5  $\mu\text{m}$  level in either the PBO-AS or PBO-600.

The fibrillar structure of this material is similar to that reported by Krause *et al.* [5] who used a detachment technique to prepare their thin sections. Microtoming enables variation in structure across the diameter of the fibres to be determined which is more difficult using the detachment method. Significant

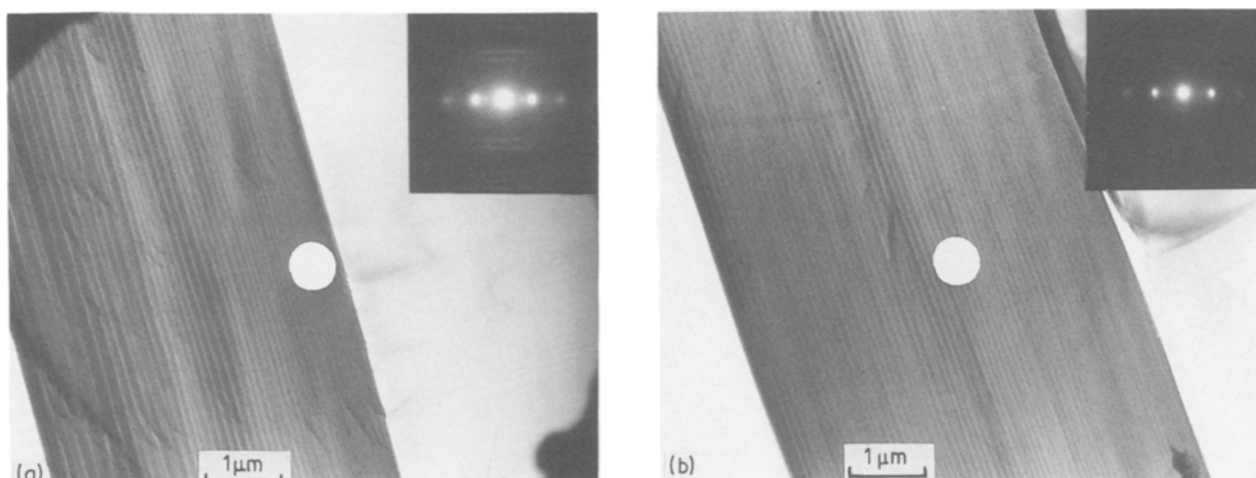


Figure 3 Transmission electron micrographs and selected-area diffraction patterns (inset) from PBO-AS: (a) skin, and (b) core.

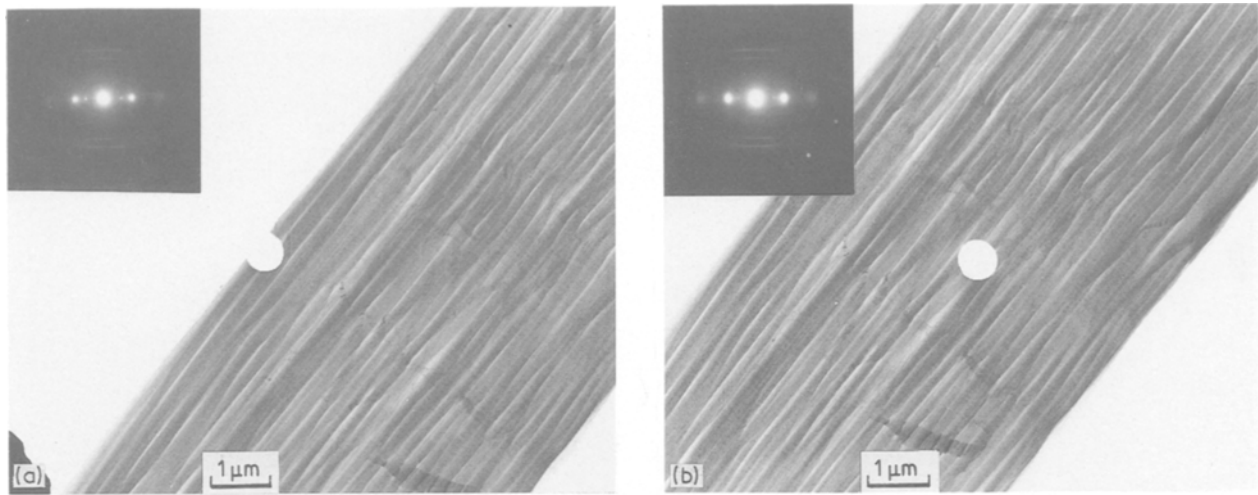


Figure 4 Transmission electron micrographs and selected-area diffraction patterns (inset) from PBO-600: (a) skin, and (b) core.

skin–core differences similar to those formed for Kevlar [18] were found for the PBO fibres. This is most pronounced for the PBO-AS material where it can be seen from Fig. 3a that the skin material has a better defined structure and a higher degree of orientation than the core material in Fig. 3b. The difference orientation was confirmed by measuring the spread intensity of the  $(hk0)$  diffraction spots perpendicular to the layer lines using a microdensitometer. The core material always showed a significantly larger spread in orientation. Quantitative data are difficult to obtain, however, because of variations in exposure level in the diffraction patterns. Better orientation in the skin was also found for the PBO-600 fibres although the core was seen to have a better defined diffraction pattern than for the PBO-AS indicating a similar level of crystallinity to that of the skin. It appears that the main effect of the heat treatment is to improve the level of crystallinity in the core regions which, of course, constitute a high proportion of the volume of the fibres. Krause *et al.* [5] showed, using dark-field electron microscopy, that this took place by an increase in the transverse dimensions of the crystallites from about 6 to 10 nm on heat treatment at elevated temperatures in air.

### 3.2. Mechanical testing

Stress–strain curves for the individual as-spun and heat-treated PBO fibres are given in Fig. 5. The mean values of Young's modulus, fracture stress and elongation to failure obtained from the three sets of specimens are given in Table I. It can be seen that the 600°C heat treatment produces an increase in the modulus of the as-spun fibres by almost a factor of 2. This is consistent with the improvement in structural order described in Section 3.1 and by Krause *et al.* [5] earlier. Our value of 250 GPa for the modulus of the PBO-600 is significantly lower than that of 370 GPa reported by previous workers for PBO [5]. However, it has not been corrected for end effects and there may also be differences in the preparation methods of the fibres used in different studies. Nevertheless, Table I shows that PBO potentially gives fibres which have somewhat better moduli than those of PBT [5, 8].

It can also be seen from Table I that the heat treatment leads to a reduction in the elongation to failure of the fibres. It appears that the 650°C treatment may have caused significant degradation because there is both a dramatic reduction in the elongation to failure and fibre strength. The results in Fig. 5 and Table I imply that from the limited information available, the

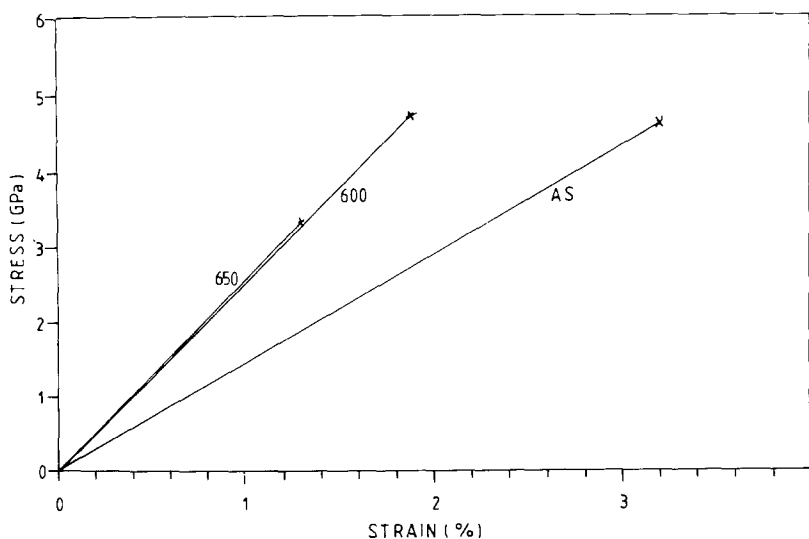


Figure 5 Typical stress/strain curves for as-spun and heat-treated PBO fibres.

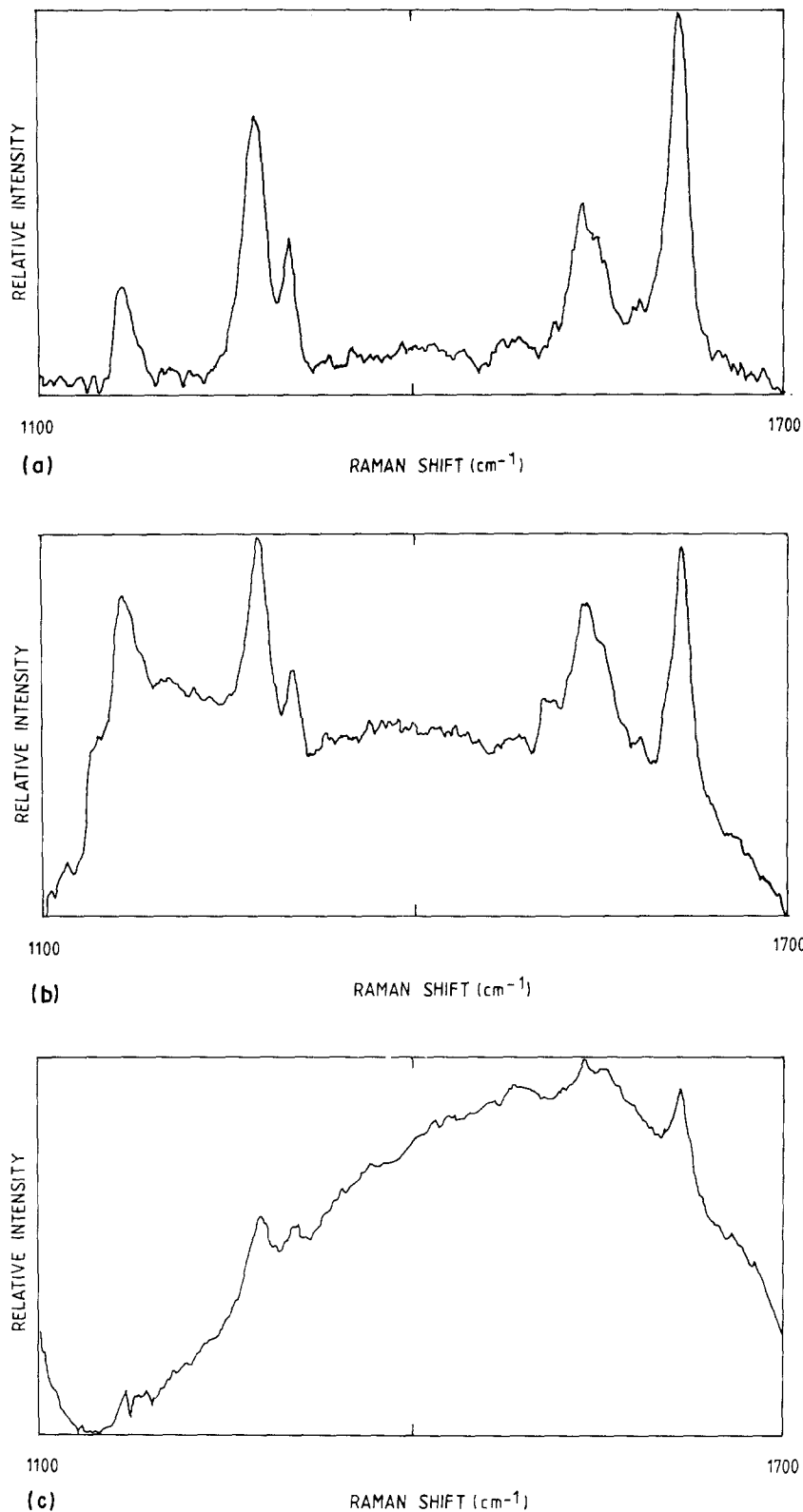


Figure 6 Raman spectra for the as-spun and heat-treated PBO fibres; (a) PBO-AS, (b) PBO-600; (c) PBO-650.

heat treatment at 600°C gives better overall fibre mechanical properties than treatment at 650°C.

In previous studies with PBT fibres [8] it was found that the as-spun fibres yielded at 0.8% strain. However, in this study of PBO the stress-strain curves were

found to be approximately linear and no yield or inelastic behaviour was found. This could be due to differences in structure between PBO and PBT but it is more likely due to differences in fibre preparation methods for the two materials.

TABLE I Dependence of the modulus ( $E$ ), tensile strength ( $\sigma_f$ ) and strain to failure ( $e_f$ ) upon heat treatment for PBO fibres

PBO fibres	$E$ (GPa)	$\sigma_f$ (GPa)	$e_f$ (%)
AS	$144 \pm 23$	$4.6 \pm 0.5$	$3.2 \pm 0.4$
600	$250 \pm 20$	$5.1 \pm 0.6$	$1.9 \pm 0.3$
650	$262 \pm 25$	$3.4 \pm 0.5$	$1.3 \pm 0.3$

### 3.3. Raman microscopy

It was possible to obtain Raman spectra readily from the PBO fibres using a relatively low power laser. This is because the microscope both concentrates the laser beam on to a small spot giving over  $10^9 \text{ W m}^{-2}$  from a 10 mW laser and is very efficient at collecting the scattered light. Typical spectra for the as-spun and

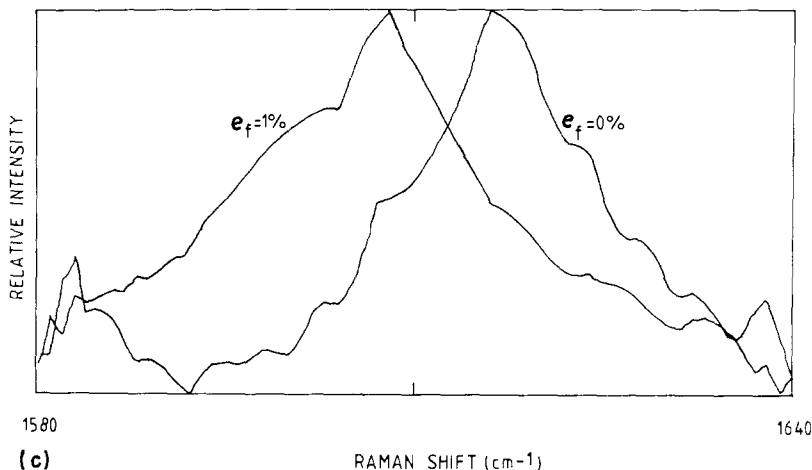
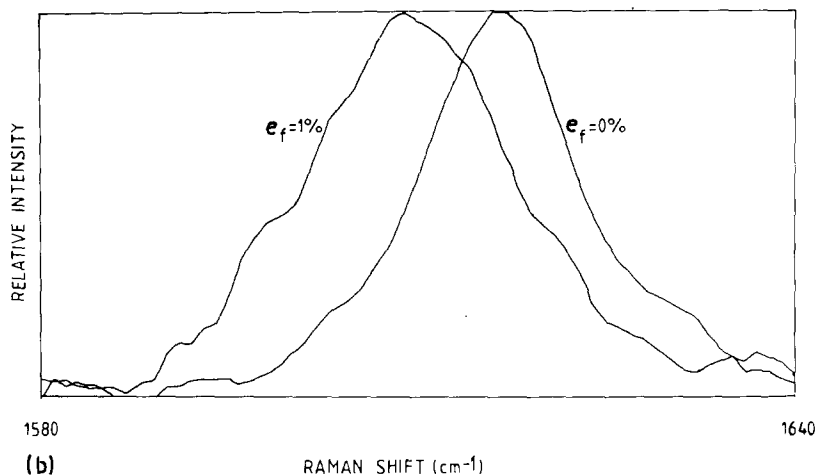
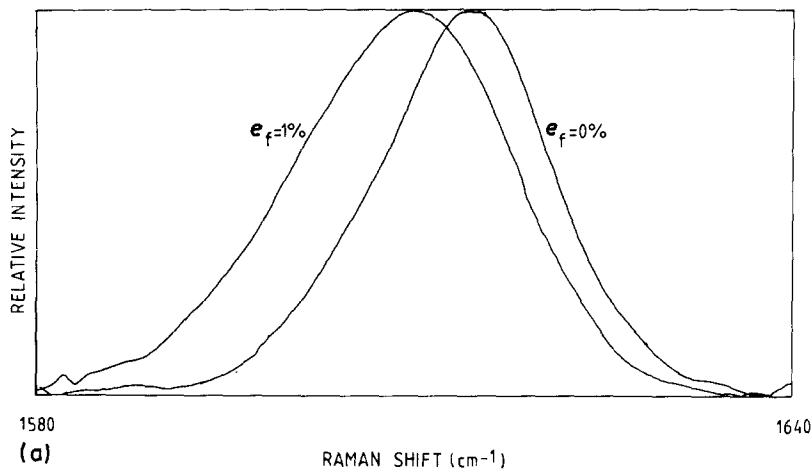


Figure 7 Raman spectra for the as-spun and heat-treated PBO fibres around  $1600\text{ cm}^{-1}$  before and after deformation to 1% strain. (1) PBO-AS, (b) PBO-600, (c) PBO-650.

heat-treated fibres are shown in Fig. 6 and it can be seen that the spectra consist of a few well-defined peaks on a fluorescent background. The level of the fluorescence can be seen to increase with the temperature of heat treatment until it virtually swamps the Raman bands for the spectrum of the PBO-650 material shown in Fig. 6c. This increase in fluorescence may be indicative of the PBO undergoing degradation during the heat treatment at  $650^\circ\text{C}$  which could also lead to the reduction in strength measured by mechanical testing (Table I).

It can be seen from Fig. 6 that there are at least five principal bands found in the Raman spectrum of PBO between  $1100$  and  $1700\text{ cm}^{-1}$ . It has not been possible to assign them all to molecular vibrations due to the

lack of Raman studies upon model materials and of theoretical analyses. This study has been concerned with the effect of deformation upon the positions of the three most intense bands which are at  $1280$ ,  $1540$  and  $1615\text{ cm}^{-1}$ .

### 3.4. Effect of deformation upon Raman spectra

Fig. 7 shows the spectra of the three types of PBO fibre studied in the  $1580$  to  $1640\text{ cm}^{-1}$  region both before deformation and at a strain of approximately 2%. It can be seen that for each of the materials the  $1615\text{ cm}^{-1}$  band shifts to lower frequency with applied strain. It is also apparent that the spectra increase in noise with heat treatment due to an increase in

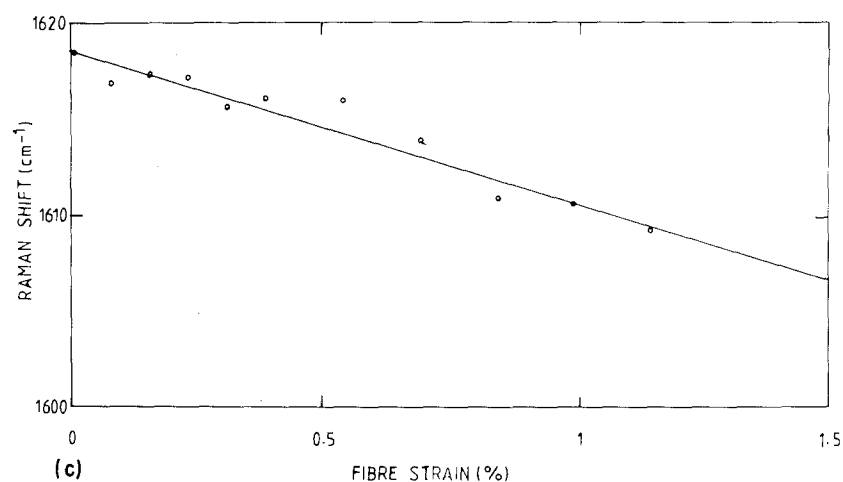
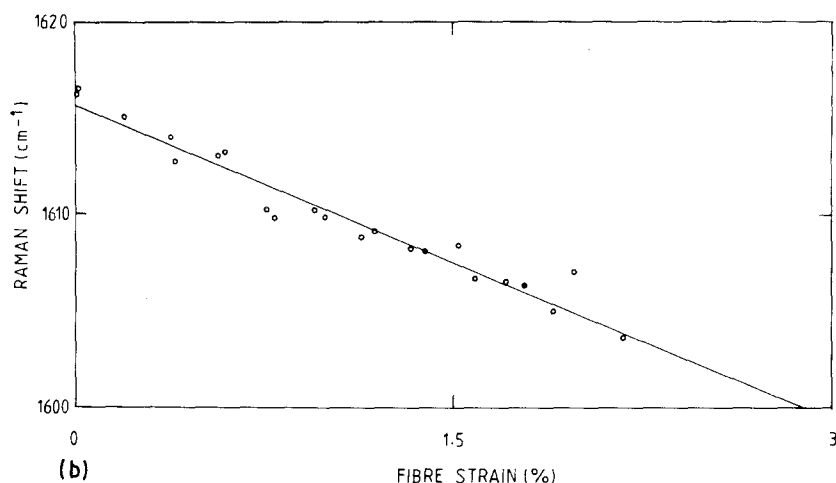
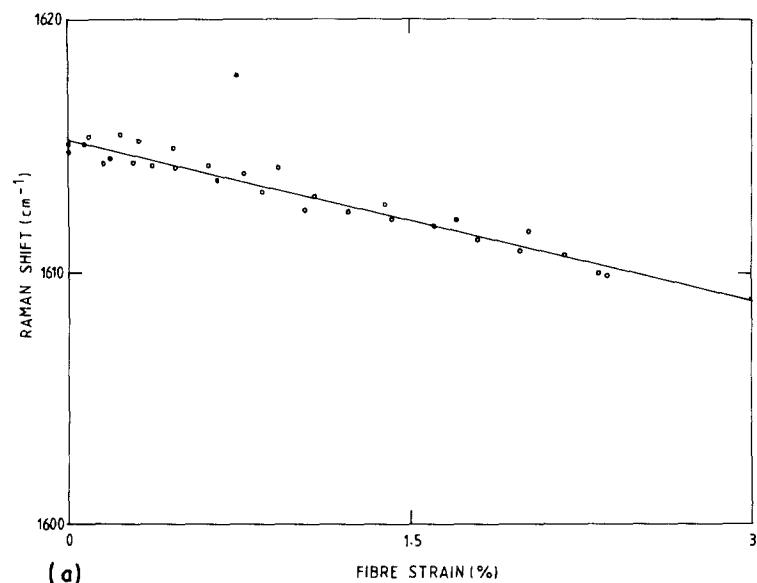


Figure 8 Dependence of the position of the  $1615\text{ cm}^{-1}$  Raman band upon applied strain for the as-spun and heat-treated PBO fibres. (a) PBO-AS, (b) PBO-600, (c) PBO-650.

fluorescent background. In each case there is some peak broadening during deformation. The effect of deformation upon the peak position for the  $1615\text{ cm}^{-1}$  band is shown in Fig. 8 for the three types of fibre. Each type of fibre exhibits a linear shift in the Raman frequency with strain until failure of the fibre takes place. The slopes of these lines for the  $1615\text{ cm}^{-1}$  bands, are listed in Table II and it can be seen that the rate of shift is significantly higher for the heat-treated fibres than for the PBO-AS. No change in slope in the lines in Fig. 8 was detected even for the PBO-AS, indicating that the fibres did not yield. This should be

contrasted with the behaviour of as-spun PBT fibres which were found to yield at a strain of about 1% [8]. The lack of any yield (as observed by Raman microscopy) is consistent with the stress-strain curves in Fig. 5. The difference between as-spun PBO and PBT could be due either to a fundamental difference of the deformation mechanisms or variations in the method of manufacture.

Although band assignments have yet to be made for PBO it is likely that the  $1615\text{ cm}^{-1}$  band is due principally to stretching of the phenyl rings using the analogy of the  $1610\text{ cm}^{-1}$  band in aromatic polyamides

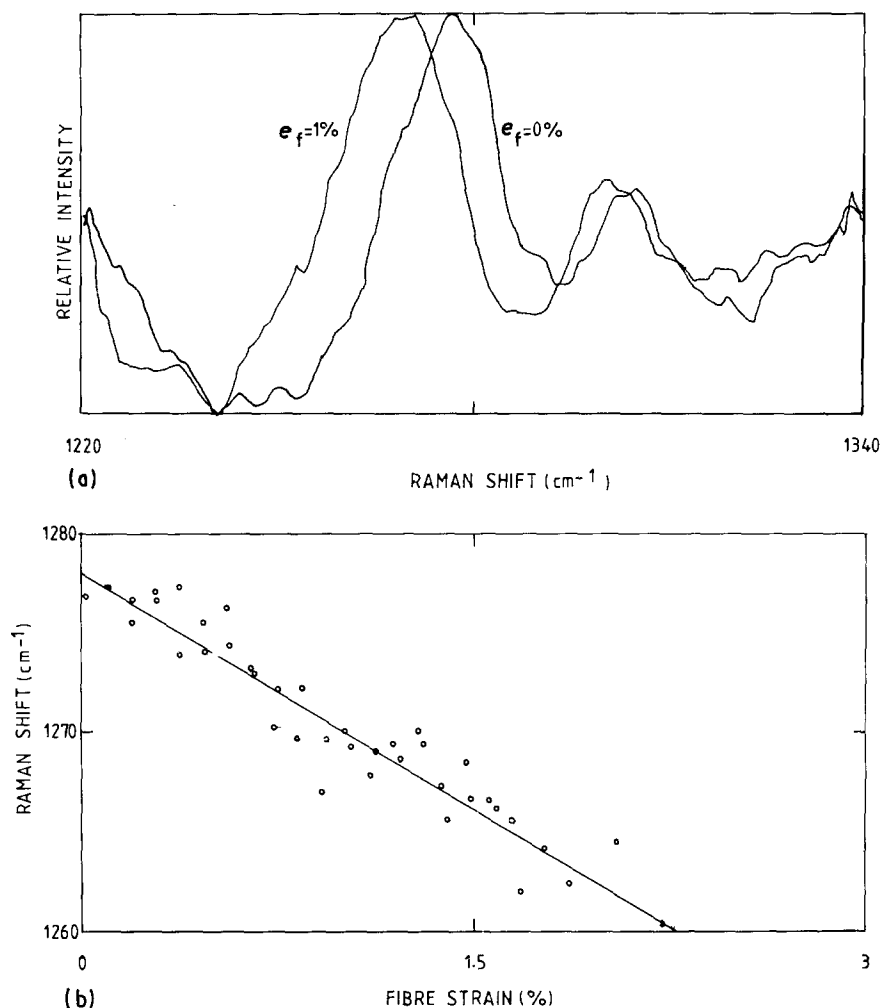


Figure 9 (a) Raman spectra for the PBO-600 fibre around  $1280\text{ cm}^{-1}$  before and after a strain of 1%. (b) Dependence of the position of the  $1280\text{ cm}^{-1}$  band upon applied strain for PB-600.

[15]. It should also be noted that there is a similarly-assigned band in PBT at  $1600\text{ cm}^{-1}$  [8].

A shift in the position of the other Raman bands with applied strain was also found for the three types of fibre. An example of this is given in Fig. 9 for PBO-600 where the spectrum in the region  $1220$  to  $1340\text{ cm}^{-1}$  is shown (Fig. 9a). It can be seen that 1% strain produces a significant shift in the position of the  $1280\text{ cm}^{-1}$  band and also of the weaker band at about  $1300\text{ cm}^{-1}$ . The change in peak position of the  $1280\text{ cm}^{-1}$  band with applied strain is shown in Fig. 9b where a linear shift is observed. The slope of the line is  $-7.9\text{ cm}^{-1}/\%$  strain and this is significantly higher than for the other bands in PBO-600. The variation in position of the  $1540\text{ cm}^{-1}$  band for PBO-600 with applied strain is shown in Fig. 10. The data are rather scattered due to the relative weakness of the  $1540\text{ cm}^{-1}$  band and the high level of fluorescence in PBO-600 (Fig. 6b). Nevertheless there is a significant shift and the slope of the line is given in Table II.

As well as finding a shift in the peak positions in the Raman spectra, significant broadening of the peaks is observed during deformation as can be seen in Figs 7 and 9a. This shows that within the individual PBO fibres the molecules are experiencing different levels of stress. There is an average level of stress but some molecules appear to be overstressed and others understressed. Work is currently underway to evaluate this effect and to relate it to the structure of the fibres.

### 3.5. Sensitivity of Raman bands to strain

The sensitivity of the Raman bands in PBT fibres was discussed in an earlier publication [8]. The data in Table II show that, as for PBT, the rates of shift are higher for the heat-treated fibres than for the as-spun fibres. Fig. 11 is a plot of the rate of shift (in  $\text{cm}^{-1}/\%$  strain) as a function of fibre modulus. This shows a similar behaviour to PBT [8] and aramid fibres [10]. The increase in modulus, due to better order and orientation, leads to the polymer molecules taking

TABLE II Peak position ( $\nu$ ) and strain sensitivity ( $\Delta\nu$ ) of the main Raman bands in PBT fibres

Band ( $\text{cm}^{-1}$ )	PBO					
	AS		600		650	
	$\nu$ ( $\text{cm}^{-1}$ )	$\Delta\nu$ ( $-\text{cm}^{-1}/\%$ strain)	$\nu$ ( $\text{cm}^{-1}$ )	$\Delta\nu$ ( $-\text{cm}^{-1}/\%$ strain)	$\nu$ ( $\text{cm}^{-1}$ )	$\Delta\nu$ ( $-\text{cm}^{-1}/\%$ strain)
1615	1615	-2.1	1615	-5.4	1618	-7.9
1540	1537	-	1537	-4.2	1551	-
1280	1274	-	1280	-7.9	1277	-

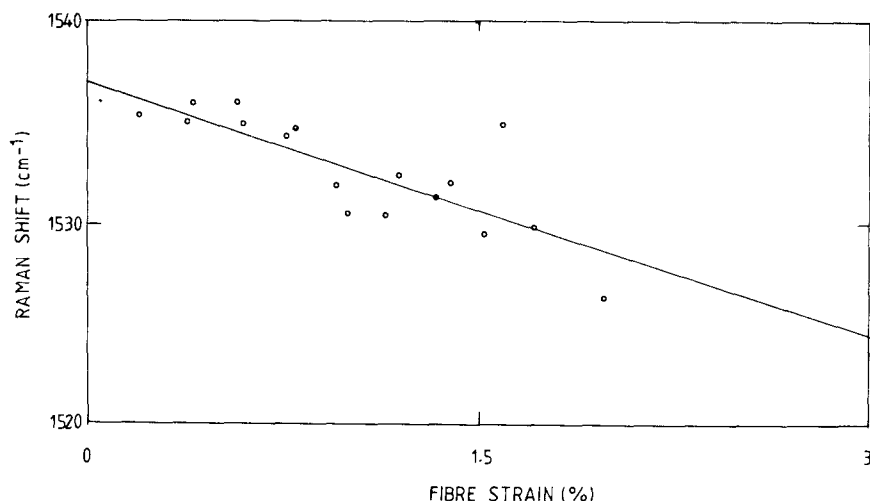


Figure 10 Dependence of the position of the  $1540\text{cm}^{-1}$  band upon applied strain for the PBO-600 fibres.

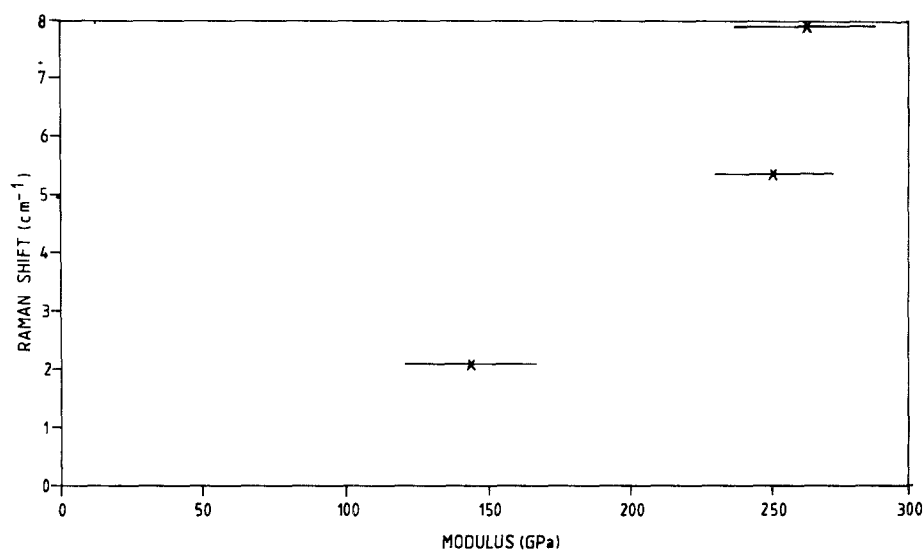


Figure 11 Rate of shift of the  $1615\text{cm}^{-1}$  band for PBO-600 fibres.

higher levels of stress at a given strain and this results in a larger change in the frequency at a given level of strain.

It now appears that this phenomenon in a general effect in most types of high modulus fibres such as PBT [8], aramids [9, 10], polydiacetylenes [6, 7], graphite [11] and even ceramics such as silicon carbide [12]. The technique we have used gives a direct demonstration of molecular deformation by backbone stretching in these high-performance fibres. As well as giving an important insight into these molecular deformation processes within fibres, Raman microscopy is an excellent technique for following the micromechanics of deformation of the fibres within composites [13–16]. Work is currently continuing in this area with PBO and PBT composites and a wide variety of other fibre-composite systems.

### Acknowledgements

The work was supported by Research grants from the SERC and the United States Airforce European Research Office.

### References

- J. R. SCHAEFGEN, in "Strength and Stiffness of Polymers", edited by A. E. Zachariades and R. S. Porter (Marcel Dekker, New York, 1983) p. 327.
- J. R. SCHAEFGEN, T. I. BAIR, J. W. BALLOU, S. L. KWOLEK, P. W. MORGAN, M. PANAR and J. ZIMMERMAN, in "Ultra-High Modulus Polymers", edited by A. Ciferri and I. M. Ward (Applied Science, London, 1979) p. 173.
- S. R. ALLEN, A. G. FILIPPOV, R. J. FARRIS and E. L. THOMAS, in "Strength and Stiffness of Polymers", edited by A. E. Zachariades and R. S. Porter (Marcel Dekker, New York, 1983) p. 357.
- S. R. ALLEN, R. J. FARRIS and E. L. THOMAS, *J. Mater. Sci.* **20** (1985) 2727.
- S. J. KRAUSE, T. B. HADDOCK, D. L. VEZIE, P. G. LENHERT, W-F. HWANG, G. E. PRICE, T. E. HELMINIAK, J. F. O'BRIEN and W. W. ADAMS, *Polymer* **29** (1988) 1354.
- D. N. BATCHELDER and D. BLOOR, *J. Polym. Sci. Polym. Phys. Edn* **17** (1979) 569.
- C. GALIOTIS, R. J. YOUNG and D. N. BATCHELDER, *ibid.* **21** (1983) 2483.
- R. J. DAY, I. M. ROBINSON, M. ZAKIKHANI and R. J. YOUNG, *Polymer* **28** (1987) 1833.
- C. GALIOTIS, I. M. ROBINSON, R. J. YOUNG, B. J. E. SMITH and D. N. BATCHELDER, *Polym. Commun.* **26** (1985) 354.
- S. VAN DER ZWAAG, M. G. NORTHOLT, R. J. YOUNG, I. M. ROBINSON, C. GALIOTIS and D. N. BATCHELDER, *ibid.* **28** (1987) 277.
- I. M. ROBINSON, M. ZAKIKHANI, R. J. DAY, R. J. YOUNG and C. GALIOTIS, *J. Mater. Sci. Lett.* **6** (1987) 1212.
- R. J. DAY, V. PIDDOCK, R. TAYLOR, R. J. YOUNG and M. ZAKIKHANI, *J. Mater. Sci.* **24** (1989) 2898–2902.
- C. GALIOTIS, R. J. YOUNG, P. H. J. YEUNG and D. N. BATCHELDER *ibid.* **19** (1984) 3640.
- I. M. ROBINSON, R. J. YOUNG, C. GALIOTIS and D. N. BATCHELDER, *ibid.* **22** (1987) 3642.

15. C. GALIOTIS, I. M. ROBINSON, D. N. BATCHELDER and R. J. YOUNG, in "Engineering Applications of New Composites", edited by S. A. Paipetis and G. C. Papanicolaou (Omega Scientific, Wallingford, 1988) p. 409.
16. R. J. YOUNG, R. J. DAY, M. ZAKIKHANI and I. M. ROBINSON, *Comp. Sci. Tech.*, 243.
17. C. GALIOTIS, J. A. PEACOCK, D. N. BATCHELDER and I. M. ROBINSON, *Composites* **19** (1988) 321.
18. M. G. DOBB, D. J. JOHNSON and B. P. SAVILLE, *J. Polym. Sci. Polym. Phys. Edn* **15** (1977) 2201.
19. J. R. MINTER, K. SHIMAMURA and E. L. THOMAS, *J. Mater. Sci.* **16** (1981) 3303.
20. J. A. ODELL, A. KELLER, E. D. T. ATKINS and M. J. MILES, *ibid.* **18** (1981) 3039.

*Received 6 January  
and accepted 31 January 1989*